Electronic Supplementary Material (ESI) for New Journal of Chemistry.

Supporting material

Figures

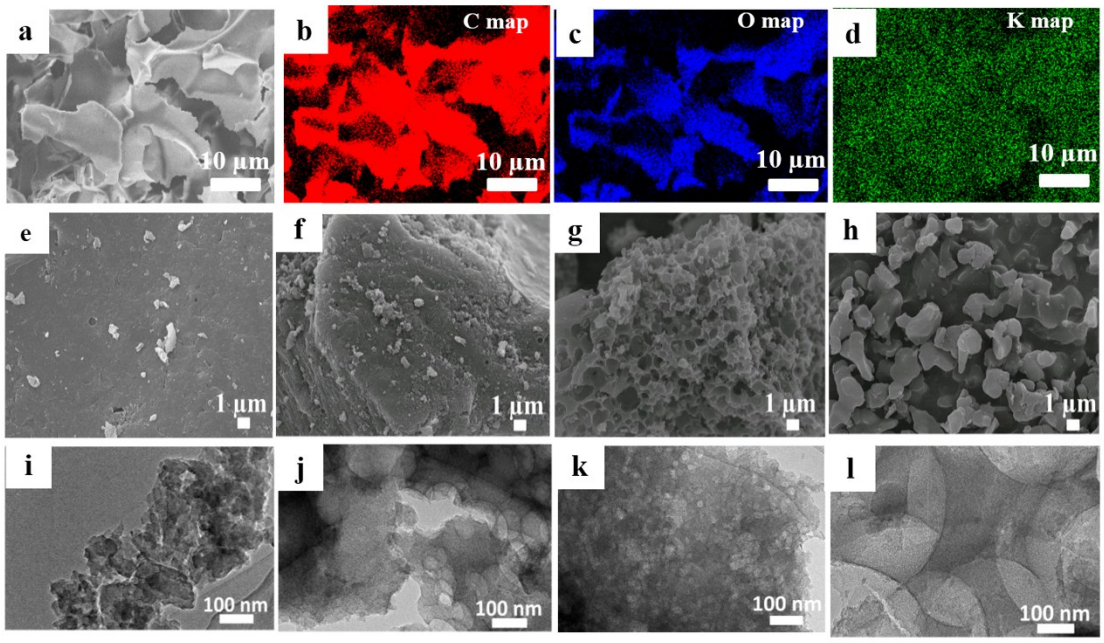

Figure S1. (a) SEM image and EDS (b) C, (c) O, and (d) K mapping of aT . Typical SEM images of (e) TC, (f) aTC-0.2, (g) aTC-0.4, and (h) aTC-0.8. Typical TEM images of (i) TC, (j) aTC-0.2, (k) aTC-0.4, and (l) aTC-0.8.

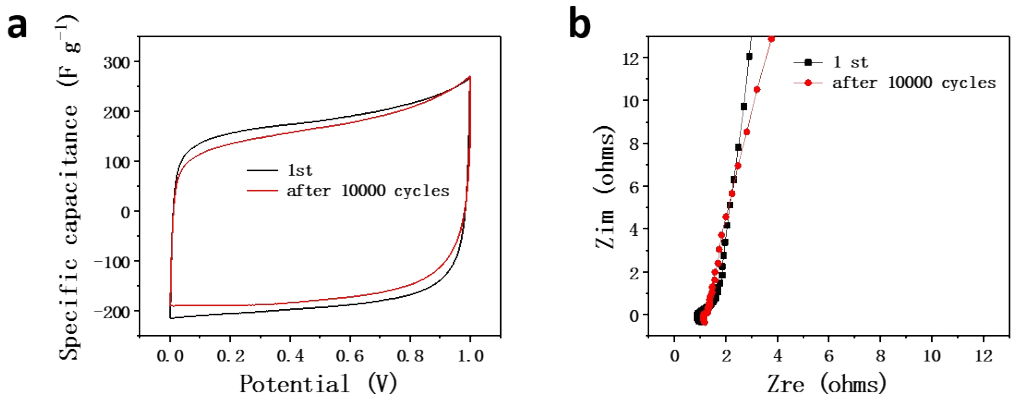

Figure S2. Electrochemical behavior of aTC-0.6 before and after 10000 cycles in 1 M H_2SO_4. (a) CV curves at 100 mV s^{-1} and (b) EIS.

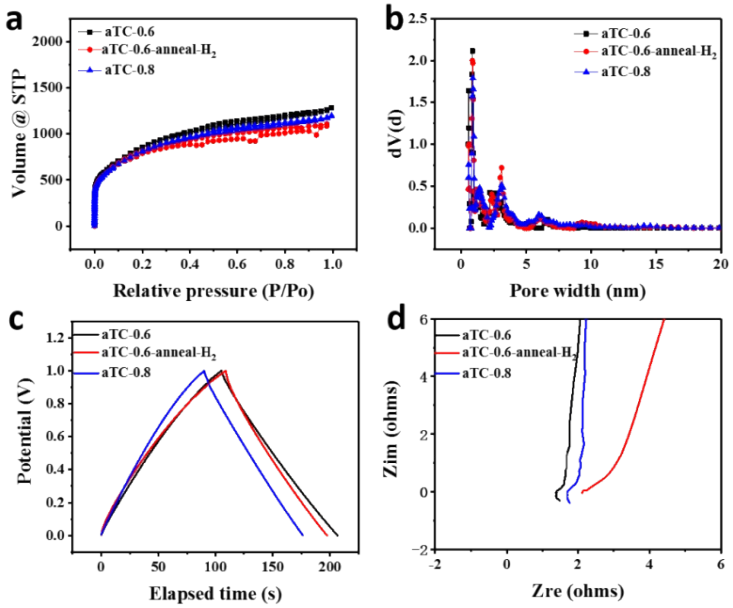

Figure S3. (a) Nitrogen adsorption-desorption isotherms of aTC-0.6, aTC-0.8 and aTC-0.6-anneal-H_2. (b) Pore size distribution of aTC-0.6, aTC-0.8 and aTC-0.6-anneal-H_2. (c) GCD plots of aTC-0.6, aTC-0.8 and aTC-0.6-anneal-H_2. (d) Nyquist plots of aTC-0.6, aTC-0.8 and aTC-0.6-anneal-H_2.

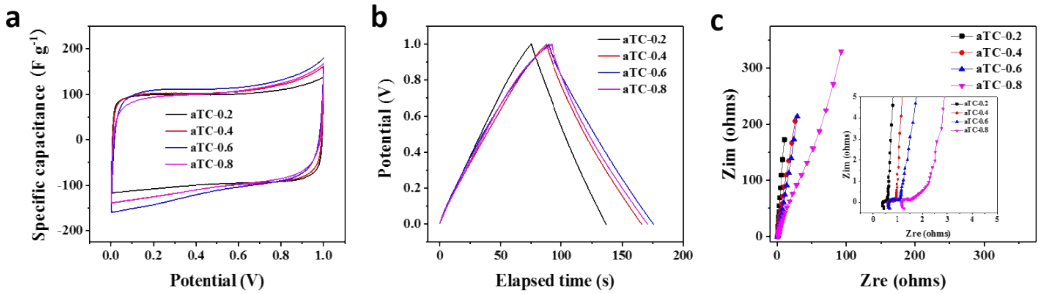

Figure S4. (a) CV curves of aTC at a scan rate of 100 mV s^{-1} in 6 M KOH. (b) GCD curves of aTCa at a current density of 1 A g^{-1} in 6 M KOH. (c) Nyquist plots of aTCa in 6 M KOH.

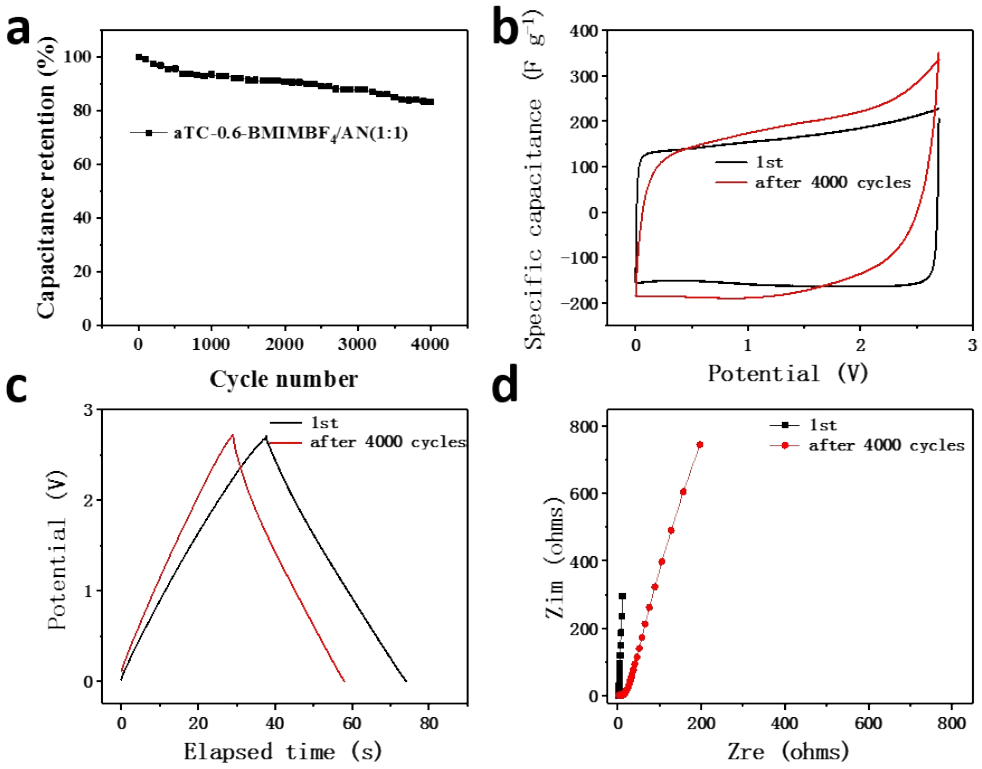

Figure S5. (a) Cycling stability of aTC-0.6 at 5 A g^{-1} in $BMIMBF_4$/AN. (b) CV curves of aTC-0.6 before and after 4000 cycles. (c) GCD curves of aTC-0.6 before and after 4000 cycles. (d) Nyquist plots of aTC-0.6 before and after 4000 cycles. The inset shows the details in low-frequency region.

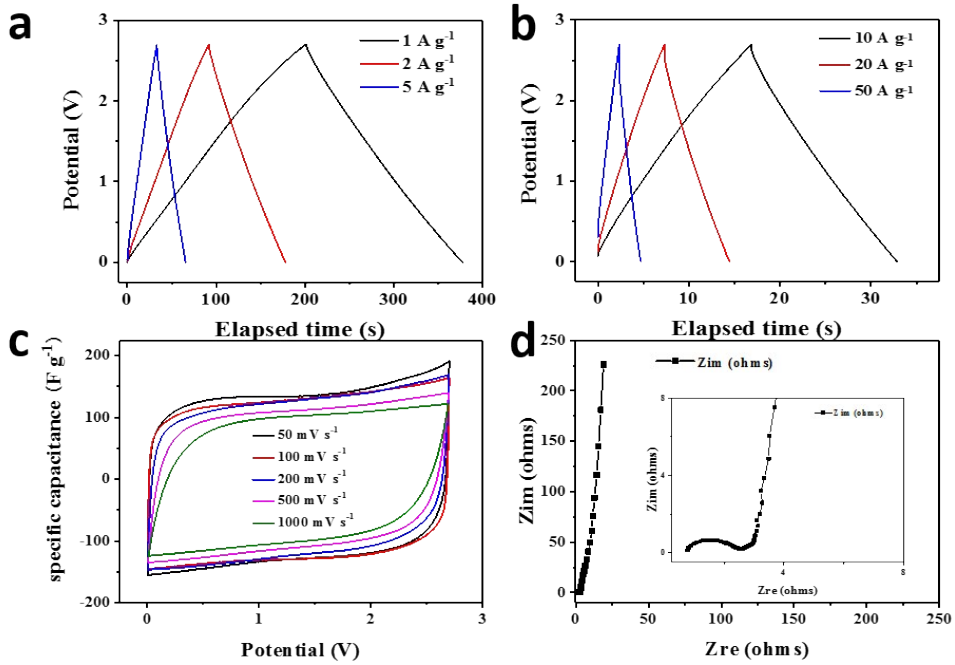

Figure S6. (a, b) GCD curves of aTC-0.6 at different current densities in 1 M $TEABF_4$/AN. (c) CV curves of aTC-0.6 at various scan rates in 1 M $TEABF_4$/AN. (d) Nyquist plots of aTC-0.6 in 1 M $TEABF_4$/AN.

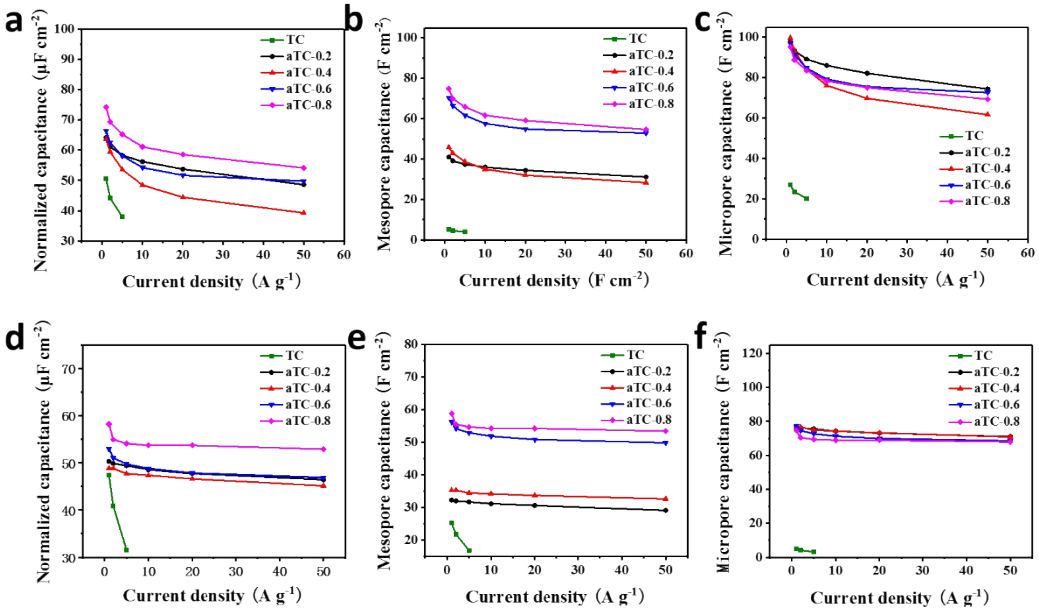

Figure S7. (a) Surface-area-normalized capacitance in 1 M H_2SO_4. (b) Capacitance attributed to the fraction of microspores in 1 M H_2SO_4. (c) Capacitance attributed to the fraction of mesopore in 1 M H_2SO_4. (d) Surface-area-normalized capacitance in 1 M $BMIMBF_4$/AN. (e) Capacitance attributed to the fraction of microspores in 1 M $BMIMBF_4$/AN. (f) Capacitance attributed to the fraction of mesopore in 1 M $BMIMBF_4$/AN.

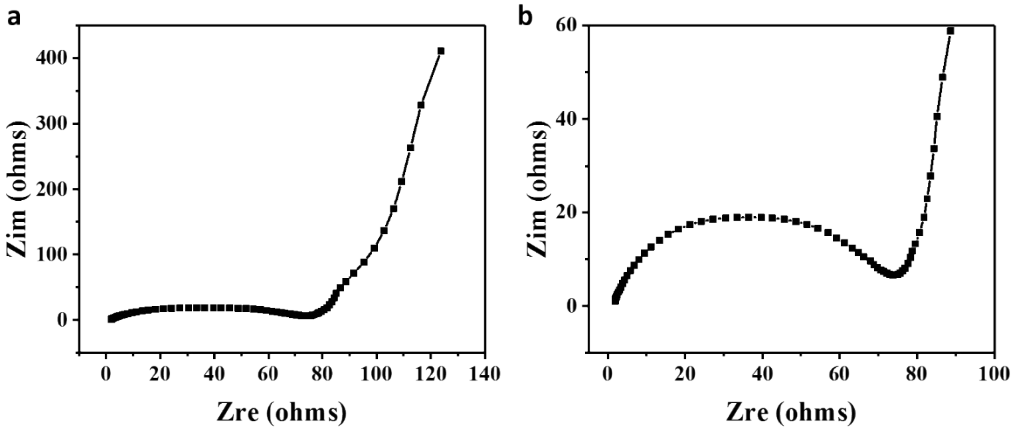

Figure S8. Nyquist plots of aTC-0.6 as LIB anode.

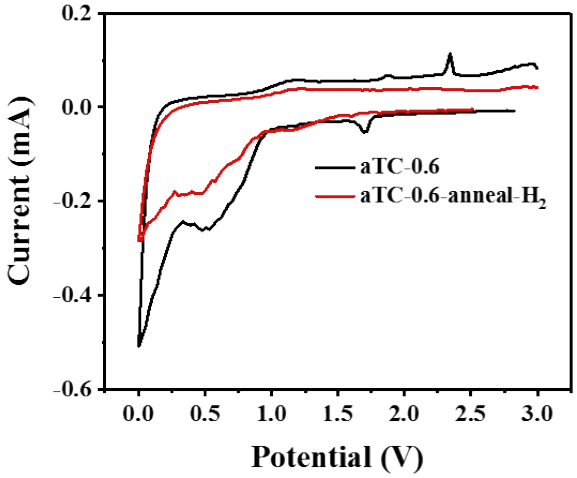

Figure S9. CV curves at 0.1 mV s^{-1} for aTC-0.6 and aTC-0.6-anneal-H_2 in 1 M $LiPF_6$/EC/DMC electrolyte.

Tables

Table S1. Elemental composition and porosity of aTC-0.6, aTC-0.8 and aTC-0.6-anneal-H_2.

Samples	aT	aT	aTC-0.6-
C (at.%)	95	95.	96.76%
N (at.%)	0.8	0.6	0.46%
O (at.%)	4.1	3.6	2.79%
S_{BET}[a] (m^2	31	24	2441
V_{total} [b]	1.8	1.6	1.56

Table S2. Weight, thickness, diameter of supercapacitor electrodes tested in different electrolytes.

Sample	2-Electrode Weight (mg)	Electrode Diameter (mm)	Electrode Thickness (μm)	Electrode Density (g cm^{-3})	Electrolyte
TC	1.77+1.74	6	61	1.02	1M H_2SO_4
aTC-0.2	1.36+1.39	8	53	0.52	1M H_2SO_4
	1.53+1.54	8	53	0.57	BMIM BF_4/AN (1:1)
aTC-0.4	1.42+1.43	8	63	0.45	1M H_2SO_4
	1.0+1.0	7	60	0.43	BMIM BF_4/AN (1:1)
aTC-0.6	1.20+1.18	8	60	0.39	1M H_2SO_4
	1.03+1.07	8	53	0.39	BMIM BF_4/AN (1:1)
	1.04+1.04	8	53	0.37	1 M TEABF_4/AN
aTC-0.8	1.14+1.18	8	60	0.38	1M H_2SO_4
	0.88+0.88	8	52	0.34	BMIM BF_4/AN (1:1)

Table S3. Comparison of the supercapacitor performance of different carbon materials derived from biomass that have been published to the results in our work.

Carbon Sources	Activation Methods	Test	Electrolyte	Gravimetric capacitance (F g^{-1})	Ref.
Soybean curd	Thermal	2-electrode	0.5 M Na_2SO_4	166 at 0.25 A g^{-1}	1
		3-electrode	2 M KOH	215 at 0.5 A g^{-1}	
Soybean root	KOH	2-electrode	6 M KOH	268 at 0.5 A g^{-1}	2
			EMIMBF_4	239 at 1 A g^{-1}	
Bagasse waste	KOH	2-electrode	1 M Na_2SO_4	44 at 0.2 A g^{-1}	3
Corn cob	Thermal-chemical	2-electrode	0.5 M H_2SO_4	210 at 0.5 A g^{-1}	4
Shrimp shell	Template-chemical	2-electrode	6 M KOH	201 at 1 A g^{-1}	5
Soya	NaOH	2-electrode	1 M H_2SO_4	155 at 1 A g^{-1}	6

Water hyacinth	KOH	2-electrode	1 M H_2SO_4	53 at 0.1 A g^{-1}	7
Wild jujube pit	KOH	2-electrode	6 M KOH	260 at 0.5 A g^{-1}	8
Moringa oleifera stem	$ZnCl_2$	2-electrode	1 M H_2SO_4	280 at 0.1 A g^{-1}	9
Polytetrafluroethylene	Thermal-template	2-electrode	6 M KOH	201 at 0.02 A g^{-1}	10
Cattle bones	Thermal	2-electrode	EMIMBF4	258 at 5 A g^{-1}	11
Eucalyptus tree leaves	$KHCO_3$	3-electrode	1 M H_2SO_4	372 at 0.5 A g^{-1}	12
		2-electrode	1 M $LiClO_4$/PPC	71 at 2 A g^{-1}	
Water purifier	KOH	2-electrode	1 M H_2SO_4	122.8 at 1 A g^{-1}	13
Sorghum vinasse	KOH	2-electrode	1M $TEABF_4$/AN	164 at 1 A g^{-1}	14
Pine tree sawdust	KOH	2-electrode	1M $TEABF_4$/AN	146 at 0.1 A g^{-1}	15
Rice straw	KOH	2-electrode	1 M H_2SO_4	156 at 0.5 A g^{-1}	16
			1M $EMIMBF_4$/AN	80 at 0.1 A g^{-1}	
Melia azedarach stone	KOH	2-electrode	1 M H_2SO_4	232 at 1 A g^{-1}	17
carboxymethylcellulose sodium	KNO_3	2-electrode	1M $TEABF_4$/AN	149 at 1 A g^{-1}	18
Corn straw	Hydrothermal and chemical activation	2-electrode	6 M KOH	222 at 1 A g^{-1}	19
			1M $TEABF_4$/AN	202 at 1 A g^{-1}	
Bacterial cellulose	$NH_4H_2PO_4$	2-electrode	$EMIMBF_4$	188 at 1 A g^{-1}	20
			1 M H_2SO_4	204.9 at 1 A g^{-1}	
Corncob	KOH	2-electrode	1 M H_2SO_4	164 at 1 A g^{-1}	21
Tofu	KOH	2-electrode	1 M H_2SO_4	243 at 0.1 A g^{-1}	Our work
			$BMIMBF_4$/AN (1:1)	170 at 1 A g^{-1}	
			1 M $TEABF_4$/AN	130 at 1 A g^{-1}	

Table S4. Comparison of the LIB performance of different carbon materials derived from biomass that have been published to the results in our work.

Carbon Sources	**Activation Methods**	**Current/Capacity**		**Ref.**
human hair derived carbon	KOH	50 mA g^{-1}	～700 mA h g^{-1}	22
		100 mA g^{-1}	～610 mA h g^{-1}	
		3.8 A g^{-1}	181 mA h g^{-1}	
Ox horns	KOH	100 mA g^{-1}	1181 mA h g^{-1}	23
		5 A g^{-1}	304 mA h g^{-1}	
Coconut oil	H_2SO_4 and H_2O_2	100 mA g^{-1}	742 mA h g^{-1}	24
		10 A g^{-1}	321 mA h g^{-1}	
		20 A g^{-1}	226 mA h g^{-1}	
silk	$ZnCl_2$ and $FeCl_3$	100 mA g^{-1}	1913 mA h g^{-1}	25

		5 A g^{-1}	523 mA h g^{-1}	
		20 A g^{-1}	261 mA h g^{-1}	
		37.2 A g^{-1}	212 mA h g^{-1}	
Duckweed	HNO_3	100 mA g^{-1}	1308 mA h g^{-1}	26
		1 A g^{-1}	630 mA h g^{-1}	
Cattle bones	Thermal	1 A g^{-1}	1230 mA h g^{-1}	11
Shrimp shell	Template-chemical	100 mA g^{-1}	1507 mAh g^{-1}	5
		500 mA g^{-1}	1014 mAh g^{-1}	
Algae-enteromorpha	KOH	100 mA g^{-1}	1709 mA h g^{-1}	27
Tofu	KOH	100 mA g^{-1}	2120 mA h g^{-1}	Our work
		1 A g^{-1}	900 mA h g^{-1}	

Reference

1. G. Ma, F. Ran, H. Peng, K. Sun, Z. Zhang, Q. Yang and Z. Lei, *RSC Advances*, 2015, **5**, 83129-83138.
2. N. Guo, M. Li, Y. Wang, X. Sun, F. Wang and R. Yang, *ACS applied materials & interfaces*, 2016, **8**, 33626-33634.
3. H. Feng, H. Hu, H. Dong, Y. Xiao, Y. Cai, B. Lei, Y. Liu and M. Zheng, *Journal of Power Sources*, 2016, **302**, 164-173.
4. M. Genovese, J. Jiang, K. Lian and N. Holm, *Journal of Materials Chemistry A*, 2015, **3**, 2903-2913.
5. F. Gao, J. Qu, C. Geng, G. Shao and M. Wu, *Journal of Materials Chemistry A*, 2016, **4**, 7445-7452.
6. M. Rana, K. Subramani, M. Sathish and U. K. Gautam, *Carbon*, 2017, **114**, 679-689.
7. K. Zheng, Y. Li, M. Zhu, X. Yu, M. Zhang, L. Shi and J. Cheng, *Journal of Power Sources*, 2017, **366**, 270-277.
8. K. Sun, S. Yu, Z. Hu, Z. Li, G. Lei, Q. Xiao and Y. Ding, *Electrochimica Acta*, 2017, **231**, 417-428.
9. Y. Cai, Y. Luo, H. Dong, X. Zhao, Y. Xiao, Y. Liang, H. Hu, Y. Liu and M. Zheng, *Journal of Power Sources*, 2017, **353**, 260-269.
10. W. Li, S. Liu, N. Pan, F. Zeng, Y. Liu, M. Zheng and Y. Liang, *Journal of Power Sources*, 2017, **357**, 138-143.
11. J. Niu, R. Shao, J. Liang, M. Dou, Z. Li, Y. Huang and F. Wang, *Nano Energy*, 2017, **36**, 322-330.
12. A. K. Mondal, K. Kretschmer, Y. Zhao, H. Liu, C. Wang, B. Sun and G. Wang, *Chemistry-A European Journal*, 2017, **23**, 3683-3690.
13. G. Li, Q. Li, J. Ye, G. Fu, J. Han and Y. Zhu, *Journal of Solid State Electrochemistry*, 2017, 1-9.
14. C. Shi, L. Hu, K. Guo, H. Li and T. Zhai, *Advanced Sustainable Systems*, 2017, **1**.
15. X. Wang, Y. Li, F. Lou, M. E. M. Buan, E. Sheridan and D. Chen, *RSC Advances*, 2017, **7**, 23859-23865.
16. N. Sudhan, K. Subramani, M. Karnan, N. Ilayaraja and M. Sathish, *Energy & Fuels*, 2016, **31**, 977-985.
17. C. Moreno-Castilla, H. García-Rosero and F. Carrasco-Marín, *Materials*, 2017, **10**, 747.
18. D. Wang, S. Liu, L. Jiao, G. Fang, G. Geng and J. Ma, *Carbon*, 2017, **119**, 30-39.
19. Y. Lu, S. Zhang, J. Yin, C. Bai, J. Zhang, Y. Li, Y. Yang, Z. Ge, M. Zhang and L. Wei, *Carbon*, 2017, **124**, 64-71.
20. L. F. Chen, Z. H. Huang, H. W. Liang, H. L. Gao and S. H. Yu, *Advanced Functional Materials*, 2014, **24**, 5104-5111.
21. M. Karnan, K. Subramani, P. K. Srividhya and M. Sathish, *Electrochimica Acta*, 2017, **228**, 586-596.
22. K. Saravanan and N. Kalaiselvi, *Carbon*, 2015, **81**, 43-53.
23. J. Ou, Y. Zhang, L. Chen, Q. Zhao, Y. Meng, Y. Guo and D. Xiao, *Journal of Materials Chemistry A*, 2015, **3**, 6534-6541.
24. R. R. Gaddam, D. Yang, R. Narayan, K. Raju, N. A. Kumar and X. Zhao, *Nano Energy*, 2016,

26, 346-352.
25. J. Hou, C. Cao, F. Idrees and X. Ma, *ACS nano*, 2015, **9**, 2556-2564.
26. F. Zheng, D. Liu, G. Xia, Y. Yang, T. Liu, M. Wu and Q. Chen, *Journal of Alloys and Compounds*, 2017, **693**, 1197-1204.
27. W. Yu, H. Wang, S. Liu, N. Mao, X. Liu, J. Shi, W. Liu, S. Chen and X. Wang, *Journal of Materials Chemistry A*, 2016, **4**, 5973-5983.